Peer-reviewed version available at *Nanomaterials* **2018**, *8*, 554; doi:10.3390/nano8070554

Communication

Neurogenic Differentiation of Human Dental Pulp Stem Cells on Graphene-Polycaprolactone Hybrid Nanofibers

Hoon Seonwoo [1,†], Kyung-Je Jang [2,†], Dohyeon Lee [3], Sunho Park [3], Myungchul Lee [2], Sangbae Park [2], Jangho Kim [3,*] and Jong Hoon Chung [2,4,*]

[1] Department of Industrial Machinery Engineering, College of Life Science and Natural Resources, Sunchon National University, Sunchon 57922, Republic of Korea.
[2] Department of Biosystems & Biomaterials Science and Engineering, Seoul National University, Seoul, 151-742, Republic of Korea.
[3] Department of Rural and Biosystems Engineering, Chonnam National University, Gwangju 61186, Republic of Korea.
[2] Research Institute of Agriculture and Life Sciences, Seoul National University, Seoul, Korea
* Correspondence: rain2000@jnu.ac.kr (J.K); jchung@snu.ac.kr (J.H.C); Tel.: +82-062-530-5181; Tel.: +82-02-880-4601

Abstract: Stem cells derived from dental tissues—dental stem cells—are flavored due to their easy acquisition. Among them, dental pulp stem cells (DPSCs) extracted from the dental pulp have many advantages such as high proliferation and highly purified population. Although their ability for neurogenic differentiation has been highlighted and neurogenic differentiation using electrospun nanofibers (NFs) has been performed, graphene-incorporated NFs have never been applied for DPSC neurogenic differentiation. Here reduced graphene oxide (RGO)-polycaprolactone (PCL) hybrid electrospun NFs were developed and applied for enhanced neurogenesis of DPSCs. First, RGO-PCL NFs were fabricated by electrospinning with incorporation of RGO and alignments, and their chemical and morphological characteristics were evaluated. Furthermore, in vitro NF properties such as influence on the cellular alignments and cell viability of DPSCs were also analyzed. The influences of NFs on DPSCs neurogenesis was also analyzed. The results confirmed that an appropriate concentration of RGO promoted better DPSC neurogenesis. Furthermore, the use of random NFs facilitated contiguous junctions of differentiated cells, whereas the use of aligned NFs facilitated aligned junction of differentiated cells along the direction of NF alignments. Our findings showed that RGO-PCL NFs can be a useful tool for DPSC neurogenesis, which will help regeneration in neurodegenerative and neurodefective diseases.

Keywords: alignments, dental pulp stem cells, nanofiber, neurogenesis, reduced graphene oxide

1. Introduction

Many efforts have been made to secure stem cell sources [1]. Depending on the cell sources, the stem cells are classified as embryonic stem cells (ESCs), bone marrow-derived stem cells (BMSCs), and adipose-derived stem cells (ADSCs). However, one critical limitation for acquiring these stem cells is the long and intense nature of the acquisition processes; this necessitates a second surgery for the donor site, which increases the risk of inflammation [2, 3]. However, stem cells can be derived from exfoliated teeth, too. Unlike other stem cells, the stem cells from dental tissues, called dental stem cells, can be derived without any surgery, because deciduous teeth, wisdom teeth, or unhealthy teeth in any case need to be extracted from periodontal tissues [3]. Thus, everyone can easily acquire their own stem cells by cryopreservation of the dental stem cells after exfoliation and separation. Based on origin, the dental stem cells are classified as dental follicle stem cells (DFSCs), dental papilla stem cells (DPPSCs), periodontal ligament stem cells (PDLSCs), and dental pulp stem cells (DPSCs) [4-6]. Among all these types of dental stem cells, DPSCs extracted from the dental pulp have many

Peer-reviewed version available at Nanomaterials 2018, 8, 554; doi:10.3390/nano8070554

advantages. Unlike other stem cells, DPSCs are highly purified [7] and are highly proliferative over 50 passages. Furthermore, the DPSCs have a vast potency: in addition to differentiating into dental tissues [8], DPSCs can also differentiate into bone [9], muscle [10], cartilage [10], and even neuronal cells [11]. Due to these advantages, DPSCs have been used in various fields, such as research on immunodeficiency disease [8] and neurological diseases [12]. DPSCs have been shown to themselves differentiate into neuronal cells and regenerate to ameliorate neurological dysfunctions [13]. Their neurogenic differentiation is largely dependent on chemical factors [14]. In addition to chemical factors, micro- to nano-structural cues and electroconductive biomaterials can also affect the efficacies of neurogenic differentiation of DPSCs. However, the neurogenic differentiation of DPSCs with biomaterials inducing micro- to nano-structural cues and electroconductivity was rarely investigated.

Electrospinning is used to fabricate micro- to nanometer-sized fibers by electric and hydrostatic forces [15]. The electrospun nanofibrous membrane has been widely used in tissue engineering, because its structures are quite similar to the structures of the extracellular matrix (ECM) [16]. In addition to random nanofibers (RFs), aligned nanofibers (AFs) can also be acquired by changing the characteristics of collectors [17]. The ECM can have different tissue-specific organizations [18]. Therefore, the application of NFs resembling the specific features of the ECM has shown outstanding results [16]. Graphene is composed of 1–10-layered subsheets of graphite, which are in turn composed of SP^2-hybridized hexagonal carbon [19]. Due to its conformational and electrochemical properties, graphene has strong mechanical properties and excellent electric properties. Such mechanical and electrochemical properties are known to influence stem cell proliferation and differentiation. Graphene and its subfamily have been reported to improve osteogenesis, neurogenesis, epithelial differentiation, and cardiomyogenic differentiation of stem cells [20, 21]. Graphene oxide (GO), one of the graphene derivatives, is usually used with NFs for tissue engineering due to its hydrophilicity, low cytotoxicity, and degradability [22]. On the contrary, reduced graphene oxide (RGO), which is derived from GO by reduction of the hydroxyl or carboxyl group [23], has rarely used in combination with NFs, especially in neurogenesis. Electroconductive materials generally promote the neurogenesis of stem cells. However, because reduction of hydroxyl and carboxyl group results in the recovery of $\pi-\pi$ bonds, RGO has higher electroconductivity than GO [24]. If RGO-incorporated NFs are fabricated and applied to stem cells, the structural cues induced by the NFs and the electrochemical cues induced by RGO would synergistically enhance the differentiation of stem cells, especially for neurogenesis. However, in our knowledge, the application of RGO-incorporated NFs in the DPSC neurogenesis has never been studied.

Therefore, in this study, we developed RGO-polycaprolactone (PCL) hybrid NFs (RGO-PCL NFs) and applied them to the neurogenesis of DPSCs (Figure 1A). For evaluating the structural cues induced by the RGO-PCL NFs, RFs and AFs were independently fabricated. In addition, the concentration of RGO was logistically applied. Their morphology was evaluated using scanning electron microscopy (FE-SEM), and their structural properties were analyzed using Image J software. The chemical properties of the RGO-PCL NFs were analyzed by Raman spectroscopy. The influences of RGO and the NFs were observed by immunocytochemistry (ICC) and quantitatively analyzed. After neurogenic differentiation, the morphologies and alignments were also observed and analyzed. Finally, the potential of the RGO-PCL NFs for application in DPSC neurogenesis was addressed.

2. Materials and Methods

2.1. Fiber fabrication

Electrospun NFs were obtained by electrospinning 10 wt% polycaprolactone (molecular weight: 80 kDa) solution in chloroform/N,N-dimethyl formamide (v/v = 3/1) incorporating 0, 0.01, and 0.1% RGO. Random nanofibers (NFs) were deposited on planar plate, and aligned nanofibers (AFs) were deposited on custom-made rotating drum.

2.2. Cell culture

The DPSCs were collected at the Intellectual Biointerface Engineering Center, Dental Research Institute, College of Dentistry, Seoul National University. The cells were cultured in α-minimum essential medium (MEM) containing 10% fetal bovine serum (FBS, Welgene Inc., Republic of Korea), 10 mM ascorbic acid (L-ascorbic acid), antibiotics, and sodium bicarbonate at 37℃ in a humidified atmosphere of 5% CO_2 (Steri-Cycle 370 Incubator, Thermo Fisher Scientific. USA). The medium was changed every other day. When the cells became confluent, they were detached with 1 mL trypsin-EDTA, counted, and passaged.

2.3. Cell viability test

Cell viability was measured using a WST-1 assay (EZ-Cytox cell viability assay kit, Daeillab Service Co., LTD). Watersoluble formazan was quantified by a multiwell spectrophotometer (Victor 3, Perkin Elmer, USA), measured at 450 nm. For ICC, DPSCs (1×10^4 cells sample-1) were seeded on the substrates, and allowed to spread for 7 days in culture media at 37℃ in a humidified atmosphere containing 5% CO_2. The adhered cells were fixed with a 4% paraformaldehyde solution (Sigma-Aldrich, Milwaukee, WI) for 20 min, permeabilized with 0.2% Triton X- 100 (Sigma-Aldrich, WI, Milwaukee) for 15 min, and stained with TRITC-conjugated phalloidin (Millipore, Billerica, MA) and 4, 6-diamidino-2-phenylinodole (DAPI; Millipore, Billerica, MA) for 1 h. Focal adhesions (FAs) were stained with a monoclonal anti-vinculin antibody (1:100; Millipore, Billerica, MA) and an FITC-conjugated goat anti-mouse secondary antibody (1:500; Millipore, Billerica, MA). Images were taken using a confocal laser scanning microscope (LSM710, Carl Zeiss, Germany).

2.4. Neurogenic differentiation

Dental pulp stem cells were placed at a density of 1×10^4 cells/cm^2 and cultured for 1 weeks in Mesenchymal Stem Cell Neurogenic Differentiation Medium (C-28015, PromoCell, Germany). ICC was conducted on day 3 and day 7 to exhibit the expression of Tuj-1 and NeuN. The cultured cells were washed in phosphate buffered saline (PBS, Sigma-Aldrich, Milwaukee, WI, USA), fixed in a 4% paraformaldehyde solution (Sigma-Aldrich, Milwaukee, WI, USA) for 20 min, and permeabilized with 0.2% Triton X-100 (Sigma-Aldrich, WI, Milwaukee, USA) for 15min. Cells were incubated with anti Tuj-1 (ab1820, abcam, cambridge, the UK), anti NeuN (ab104225, abcam, cambridge, the UK), and 4, 6-diamidino-2-phrnykinodole (DAPI;Millipore, Billerica, MA, USA) for 1 h.

3. Results and Discussions

3.1. Characterization of the RGO-PCL NFs

First, the RGO-PCL NFs were characterized. The morphology of RGO-PCL NFs was assessed by SEM (Figure 1B). The RFs were disordered without any alignment, whereas the AFs were aligned along with the revolution direction of the rotating collector. The alignments of the NFs were quantitatively analyzed using Image J software. The box plot revealed that the orientations of the RFs were distributed broadly, whereas those of the AFs were concentrated in a narrow region (Figure 1C). The AFs showed significantly higher coherency than the RFs (Figure 1D). Furthermore, incorporation of RGO influenced the alignments of the NFs. One percent incorporation of RGO caused a significant decrease in the coherency of RF-1% compared with that of RF-0% and RF-0.1%. In Raman spectroscopy, the NFs 0.1% and 1% RGO exhibited D (~1450 cm^{-1}) and G peaks (~1600 cm^{-1}), the representative peaks of RGO (Figure 1E).

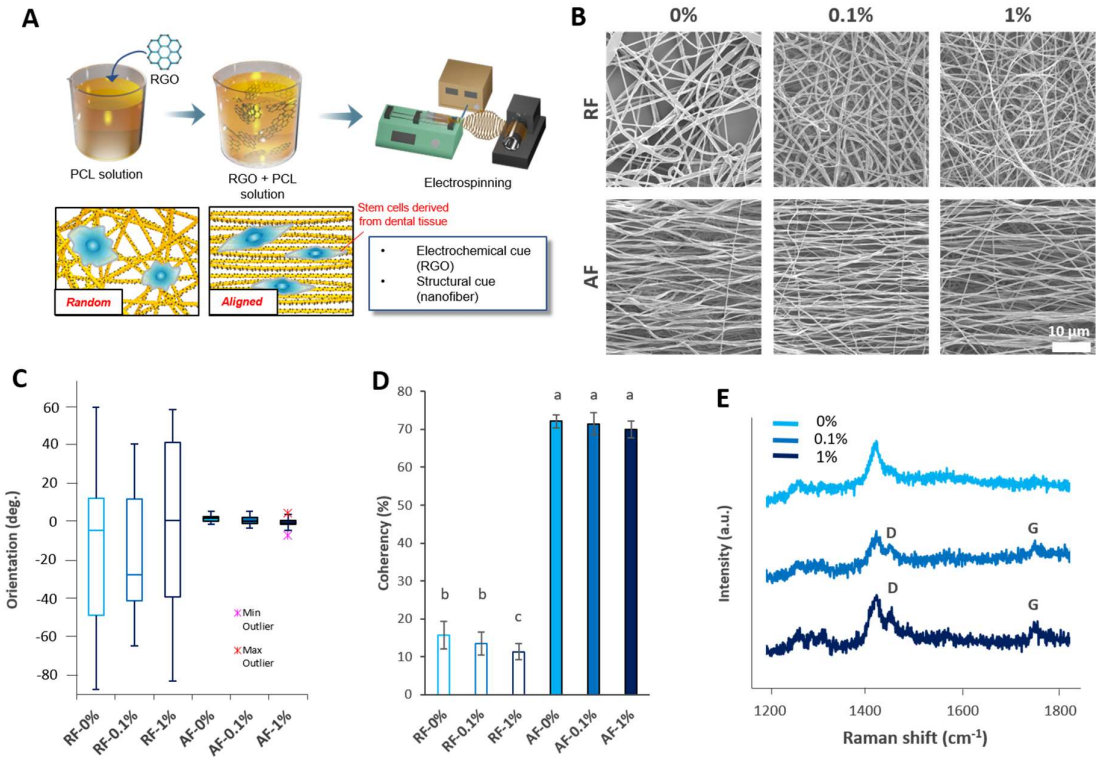

Figure 1. Characteristics of the reduced graphene oxide-polycaprolactione hybrid electrospun nanofibers (RGO-PCL NFs). (A) Study strategy. RGO was incorporated into PCL solution and sonicated for even distribution. Then, the solution was electrospun to achieve random nanofibers (RFs) and aligned nanofibers (AFs). The fabricated nanofibers were used for the neurogenic differentiation of DPSCs. (B-D) Morphological analysis. (B) Representative images of electrospun RGO-PCL NFs. (C) Orientation of the RGO-PCL NFs. The orientation of the RFs are distributed broadly, whereas those of the AFs show narrow distribution. Each of the 25 images were used for the analysis. (D) Coherency of the RGO-PCL NFs. The coherencies of AFs were significantly higher than those of RFs. Each of 25 images were used for the analysis. Error bars represent standard deviation. Same alphabets represent non-significance ($p < 0.05$). (E) Raman spectroscopy results. The 0.1% and 1% RGO-incorporated NFs exhibited D (~1450 cm^{-1}) and G peaks (~1600 cm^{-1}), the characteristic peaks of RGO. (C) XRD results. The 0.1% and 1%-incorporated NFs exhibited the characteristic peaks of RGO at approximately 23.5°. RGO, reduced graphene oxide; PCL, polycaprolactone; DPSCs, dental pulp stem cells.

3.2. Influence of the RGO-PCL NFs on DPSC behavior

After characterization of the NFs, their influence on DPSCs were assessed. Two days after seeding the DPSCs, the cellular morphologies were observed by ICC (Figure 2A). The DPSCs on the RFs were aligned randomly, whereas those on the AFs were well aligned following the orientation of the fibers. The alignments of the DPSCs according to the NFs were analyzed using image analysis. Corresponding to the alignments of NFs, the cellular alignments were randomly distributed on the RFs, whereas those on the AFs were narrow (Figure 2B). The AFs exhibited significantly higher coherency than the RFs, except for AF-1% (Figure 2C). Based on the results, the cellular alignments were confirmed to be influenced highly by NF alignments. Furthermore, high incorporation of RGO (1%) decreased cellular alignments significantly. In the characterization study, high incorporation of RGO (1%) decreased the alignments of the NFs. Therefore, it was anticipated that high incorporation of RGO (1%) decreased the alignments of NFs, which further resulted in a corresponding decrease in cellular alignments. Cell viability was also assessed (Figure 2D), and it was found that the NF

Preprints (www.preprints.org) | NOT PEER-REVIEWED | Posted: 27 June 2018 doi:10.20944/preprints201806.0452.v1

Peer-reviewed version available at Nanomaterials 2018, 8, 554; doi:10.3390/nano8070554

alignments and RGO concentration did not significantly affect cell viability on day 3, except for AF-1%; cell viability with AF-1% was significantly decreased. Based on the result, we believe that the NF alignments and high concentration of RGO (1%) negatively affect initial cell proliferation. On the contrary, the NF alignments and RGO concentation appeared to affect cell viability on day 7. Cell viability with AF-0.1% was significantly increased, whereas that with RF-0.1% and RF-1% was significantly decreased. It is well known that the incorporation of nanomaterials usually has negative effects on cell viability. Concurrently, on day 7, we found that cell viability was decreased on RF-0.1% and RF-1%. On the contrary, the cell viability on AF-1% was similar to that on RF-0%. The cell viability on AF-0.1% was further significantly higher than that on RF-0.1%. Thus, we believe that incorporation of an appropriate percentate of RGO and AFs synergically increase the viability of DPSCs.

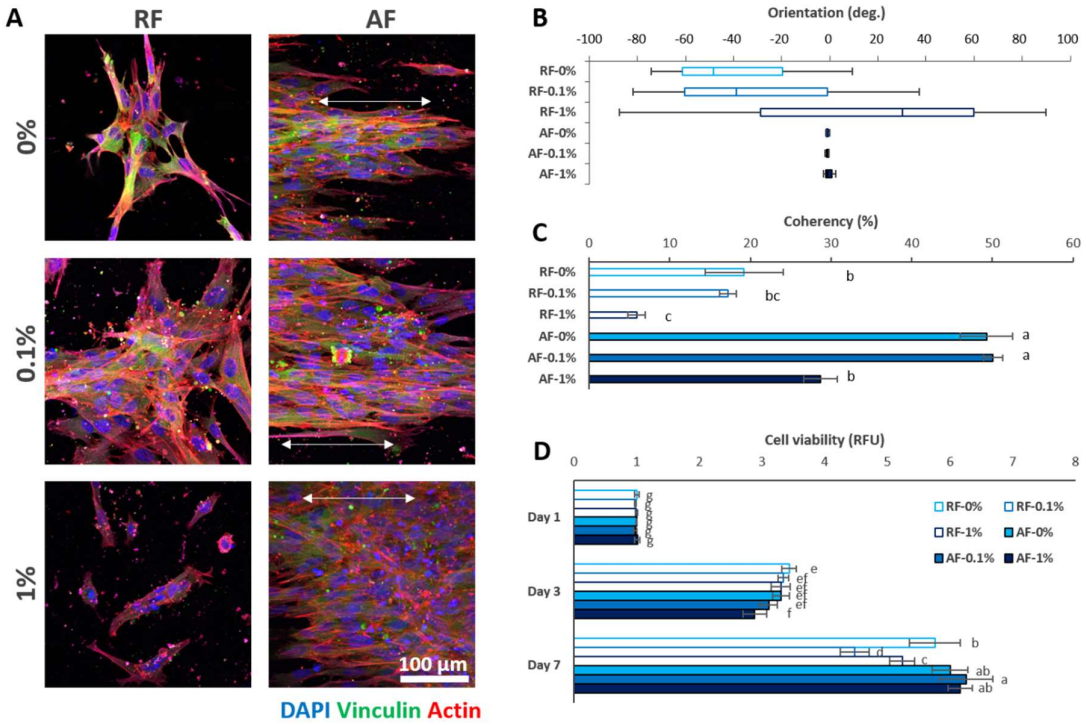

Figure 2. Effects of the RGO-PCL NFs on DPSC behavior. (A-C) Analyses of cellular morphologies. (A) ICC results 2 days after seeding. Corresponding with the NF alignments, the DPSCs on the RFs were randomly aligned, whereas those on the AFs were aligned well. In particular, vinculin, an indicator of focal adhesion, did not stain the cells on the 1% RGO-PCL NFs, which indicated that excessive RGO incorporation may be harmful to initial cell adhesion. (B) DPSC alignments. Corresponding to the RGO-PCL NFs, the cells on the RFs showed broad orientation, whereas those on the AFs showed narrow orientation. (C) Coherency of the DPSC alignments. The alignments of the DPSCs on AFs were significantly higher than those of cells on the RFs, except for AF-1%. Furthermore, the cells on NFs with high RGO incorporation (1%) showed significantly decreased coherency. Error bars indicate standard deviation. Same alphabets mean non-significant difference between samples ($p < 0.05$). (D) Cell viability of DPSCs on the RGO-PCL NFs. On day 3, cells on AF-1% showed significantly decreased viability. On day 7, cells on AF-0.1% showed significantly higher viability, whereas those on RF-0.1% and RF-1% showed significantly lower viability. Error bars indicate standard deviation. Same alphabets mean non-significant difference between samples ($p < 0.05$).

3.3. Neurogenic differentiation

The effects of RGO and NFs on the neurogenic differentiation were also observed. The DPSCs seeded on the RGO-PCL NFs were subjected to neurogenic differentiation. On days 3 and 7, the DPSCs seeded on NFs with 0.1% and 1% RGO showed apparent changes in their morphologies (Figure 3A).

In particular, NFs with 0.1% and 1% RGO resulted in high expression of Tuj1, the early marker of neurogenesis, and NeuN, the late marker of neurogenesis. In contrast, the cells on 1% group showed shorter axon-like legs. These results indicated that excessive incorporation of RGO (1%) might result in neurodegeneration of DPSCs. Therefore, incorporation of the appropriate concentration of RGO (0.1%) might promote the neurogenic differentiation of DPSCs. The alignments of the NFs also affected the orientation of the differentiated cells. The alignments of cells on the RFs were randomly distributed, whereas those on the AFs were highly organized. Based on the ICC results, we conducted image analyses to confirm the cellular alignments. The differentiated cells on the RFs exhibited randomly oriented alignments, whereas those on the AFs exhibited well-oriented alignments. The coherency also proved the result: those on the AFs showed significantly better results than those on the RFs.

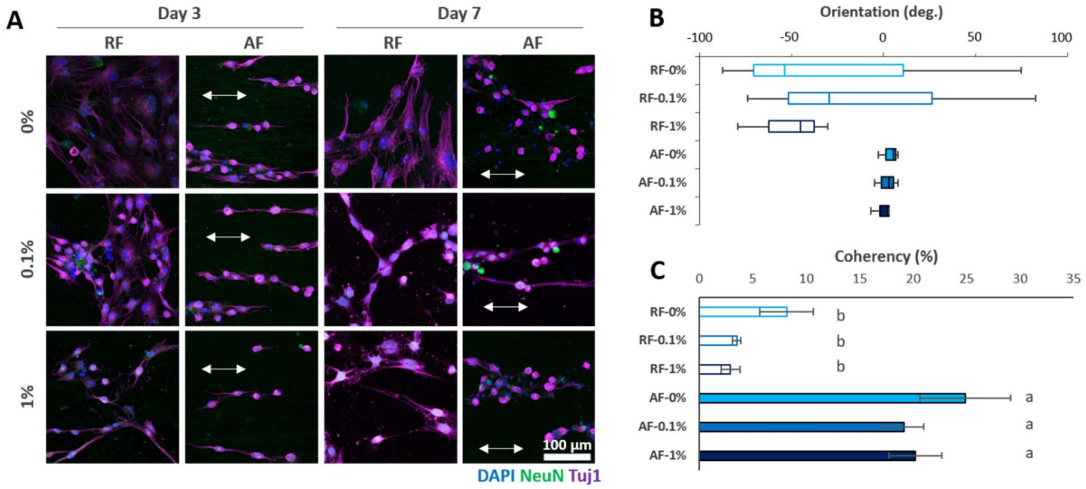

Figure 3. Neurogenic differentiation of DPSCs using RGO-PCL NFs. (A) ICC results. The RGO-incorporated NFs resulted in faster morphological transformation and early expression of Tuj1 and NeuN. The DPSCs on the RFs seemed randomly aligned, whereas those on the AFs seemed well aligned. (B) Orientation of the alignments of the differentiated cells. Corresponding to the alignments of the RGO-PCL NFs, the cells on the RFs showed broad orientation, whereas those on the AFs showed narrow orientation. (C) Coherency of the alignments of the differentiated cells. The alignments of DPSCs on the AFs were significantly higher than those of the DPSCs on the RFs, except for AF-1%. Furthermore, the cells with high RGO incorporation (1%) showed significantly decreased coherency. Error bars indicate standard deviation. Same alphabets mean non-significant difference between samples ($p < 0.05$).

The alignments of the NFs seemed to influence not only the cellular alignments, but also cellular morphologies. The cells on RF-0.1% had multipolar structures, whereas those on AF-0.1% had bipolar structures (Figure 4A). Therefore, it was proposed that the cells on RF-0.1% were connected with the neighbor cells, whereas those on AF-0.1% seemed to be connected along the direction of the fiber alignments. It is well known that nanostructures affect cellular adhesion and alignments [25]. In particular, anisotropic nanopatterns give rise to well-ordered alignments with adjacent cells [26, 27]. Cellular alignments influence not only cellular function, but also stem cell differentiation. Therefore, anisotropic nanopatterns have been used frequently in stem cell engineering, especially in neurogenic differentiation. To date, many types of techniques such as self-assembly, lithography, and electrospun NFs have been used in neurogenesis. Among them, electrospun NFs have been used widely due to their good biocompatibility and easy fabrication. Furthermore, specific cytokines or nanomaterials can be easily incorporated into the NFs, which results in enhanced functionality of the NFs. To date, GO- and RGO-incorporated NFs have been reported to enhance the viability of neuronal cells and mesenchymal stem cells, respectively. However, the influence of RGO-incorporated NFs on stem cell differentiation, especially in neurogenic differentiation, has not been studied so far. The results of our study showed that the incorporation of an appropriate concentration

Preprints (www.preprints.org) | NOT PEER-REVIEWED | Posted: 27 June 2018 doi:10.20944/preprints201806.0452.v1

Peer-reviewed version available at Nanomaterials 2018, 8, 554; doi:10.3390/nano8070554

of RGO (0.1%) increases cell viability and neurogenic differentiation. Furthermore, the alignments of the NFs influence the alignments of the DPSCs as well as the linkage of differentiated neurites. Based on these results, we suggest that the use of RF-0.1% is suitable for the regeneration of the central nervous system, whereas the use of AF-0.1% is suitable for the regeneration of the peripheral nervous system (Figure 4B).

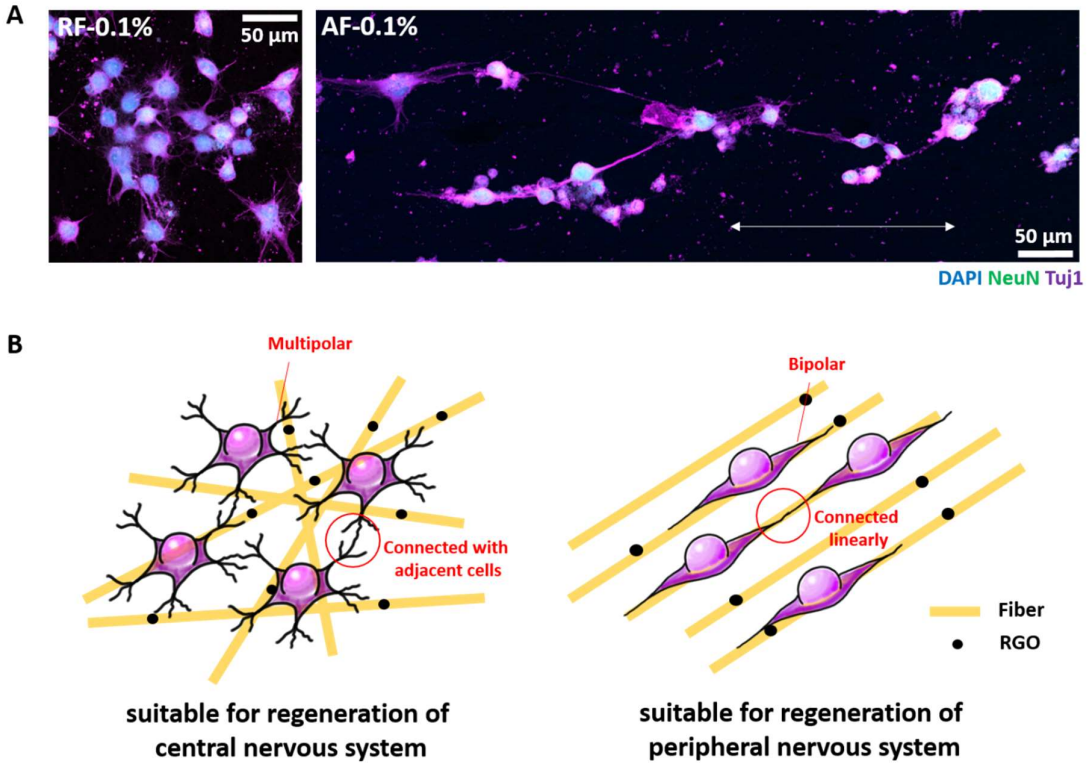

Figure 4. Effects of the RGO-PCL NF alignments on the conjunction of the differentiated DPSCs. (A) Comparison of neurites. Neurites differentiated from cells on RF-0.1% were connected with the adjacent cells, whereas those on AF-0.1% stretched and connected along the direction of the AF alignments. (B) Perspectives of the study. Because RF-0.1% can connect the differentiated cells with the adjacent cells, it can be used in the regeneration of the central nervous systems. On the other hand, AF-0.1% can be used in the regeneration of the peripheral nervous systems, because it can align and connect the differentiated cells along the direction of the AF alignments.

4. Conclusions

In this study, RGO-PCL NFs were fabricated with different alignments and RGO concentrations and applied to the neurogenesis of DPSCs. The presence of RGO was confirmed by Raman spectroscopy and XRD. The alignments of the RGO-PCL NFs directly affected the alignments of the DPSCs: the DPSCs followed the alignments of the RGO-PCL NFs. Furthermore, the combination of the alignments and RGO increased the cell viability. In the neurogenic differentiation study, incorporation of an appropriate concentration of RGO (0.1%) enhanced the neurogenesis of the DPSCs. Furthermore, the alignments of NFs seemed to correlatively affect the tissue morphologies. In conclusion, our findings indicated that the application of RGO-PCL NFs with an appropriate concentration of RGO would open the gates for the use of DPSCs in neurological therapy and neurogenesis.

Author Contributions: Study design: Hoon Seonwoo, Kyoung-Je Jang, Jong Hoon Choung. Study conduct: Hoon Seonwoo, Kyung-Je Jang, Dohyeon Lee, Sunho Park, Myungchul Lee, Sangbae Park. Data collection: Hoon Seonwoo, Kyung-Je Jang, Myungchul Lee, Sangbae Park. Data analysis: Hoon Seonwoo, Kyung-Je Jang, Dohyeon Lee, Sunho Park, Jangho Kim, Jong Hoon Chung. Data interpretation: Hoon Seonwoo, Jangho Kim,

Jong Hoon Chung. Drafting manuscript: Hoon Seonwoo, Kyoung-Je Jang, Jangho Kim, Jong Hoon Chung. Revising manuscript content: Hoon Seonwoo, Kyoung-Je Jang, Jangho Kim, Jong Hoon Chung. Approving final version of manuscript: Hoon Seonwoo, Kyung-Je Jang, Myungchul Lee, Sangbae Park, Dohyeon Lee, Sunho Park, Jangho Kim, Jong Hoon Chung takes full responsibility for the integrity of the data analysis

Funding: This work was supported by Korea Institute of Planning and Evaluation for Technology in Food, Agriculture, Forestry and Fisheries(IPET) through Agri-Bio Industry Technology Development Programy, funded by Ministry of Agriculture, Food and Rural Affairs(MAFRA)(IPET116135-3). This work was also carried out with the support of "Cooperative Research Program for Agriculture Science & Technology Development (Project No. PJ0123022016)" Rural Development Administration, Republic of Korea.

Acknowledgments: In this section you can acknowledge any support given which is not covered by the author contribution or funding sections. This may include administrative and technical support, or donations in kind (e.g., materials used for experiments).

Conflicts of Interest: The authors declare no conflict of interest.

References

1. Sart, S., Agathos, S.N., Li, Y., and Ma, T., Regulation of mesenchymal stem cell 3D microenvironment: From macro to microfluidic bioreactors. *Biotechnology journal* **2016**. *11*. 43-57.
2. Tsuji, T., Hughe, F., McCulloch, C., and Melcher, A., Effects of donor age on osteogenic cells of rat bone marrow in vitro. *Mechanisms of ageing and development* **1990**. 51. 121-132.
3. Dodson, S.A., Bernard, G.W., Kenney, E.B., and Carranza, F.A., In vitro comparison of aged and young osteogenic and hemopoietic bone marrow stem cells and their derivative colonies. *Journal of periodontology* **1996**. *67*. 184-196.
4. Jo, Y.-Y., Lee, H.-J., Kook, S.-Y., Choung, H.-W., Park, J.-Y., Chung, J.-H., Choung, Y.-H., Kim, E.-S., Yang, H.-C., and Choung, P.-H., Isolation and characterization of postnatal stem cells from human dental tissues. *Tissue engineering* **2007**. *13*. 767-773.
5. Morsczeck, C., Götz, W., Schierholz, J., Zeilhofer, F., Kühn, U., Möhl, C., Sippel, C., and Hoffmann, K., Isolation of precursor cells (PCs) from human dental follicle of wisdom teeth. *Matrix Biology* **2005**. *24*. 155-165.
6. Ikeda, E., Hirose, M., Kotobuki, N., Shimaoka, H., Tadokoro, M., Maeda, M., Hayashi, Y., Kirita, T., and Ohgushi, H., Osteogenic differentiation of human dental papilla mesenchymal cells. *Biochemical and biophysical research communications* **2006**. *342*. 1257-1262.
7. Gronthos, S., Mankani, M., Brahim, J., Robey, P.G., and Shi, S., Postnatal human dental pulp stem cells (DPSCs) in vitro and in vivo. *Proceedings of the National Academy of Sciences* **2000**. *97*. 13625-13630.
8. Demircan, P.C., Sariboyaci, A.E., Unal, Z.S., Gacar, G., Subasi, C., and Karaoz, E., Immunoregulatory effects of human dental pulp-derived stem cells on T cells: comparison of transwell co-culture and mixed lymphocyte reaction systems. *Cytotherapy* **2011**. *13*. 1205-1220.
9. Bressan, E., Ferroni, L., Gardin, C., Pinton, P., Stellini, E., Botticelli, D., Sivolella, S., and Zavan, B., Donor age-related biological properties of human dental pulp stem cells change in nanostructured scaffolds. *PLoS One* **2012**. *7*. e49146.
10. Gandia, C., Arminan, A., García-Verdugo, J.M., Lledo, E., Ruiz, A., Minana, M.D., Sanchez-Torrijos, J., Paya, R., Mirabet, V., and Carbonell-Uberos, F., Human dental pulp stem cells improve left ventricular function, induce angiogenesis, and reduce infarct size in rats with acute myocardial infarction. *Stem cells* **2008**. *26*. 638-645.
11. Nakashima, M., Iohara, K., and Murakami, M., Dental pulp stem cells and regeneration. *Endodontic Topics* **2013.** *28*. 38-50.
12. Huang, A.H.C., Snyder, B.R., Cheng, P.H., and Chan, A.W., Putative dental pulp-derived stem/stromal cells promote proliferation and differentiation of endogenous neural cells in the hippocampus of mice. *Stem cells* **2008**. *26*. 2654-2663.
13. Ishizaka, R., Hayashi, Y., Iohara, K., Sugiyama, M., Murakami, M., Yamamoto, T., Fukuta, O., and Nakashima, M., Stimulation of angiogenesis, neurogenesis and regeneration by side population cells from dental pulp. *Biomaterials* **2013**. *34*. 1888-1897.
14. Takeyasu, M., Nozaki, T., and Daito, M., Differentiation of dental pulp stem cells into a neural lineage. *Pediatric Dental Journal* **2006**. *16*. 154-162.

15. Agarwal, S., Wendorff, J.H., and Greiner, A., Progress in the field of electrospinning for tissue engineering applications. *Advanced Materials* **2009**. *21*. 3343-3351.
16. Liu, W., Thomopoulos, S., and Xia, Y., Electrospun nanofibers for regenerative medicine. *Advanced healthcare materials* **2012**. *1*. 10-25.
17. Barnes, C.P., Sell, S.A., Boland, E.D., Simpson, D.G., and Bowlin, G.L., Nanofiber technology: designing the next generation of tissue engineering scaffolds. *Advanced drug delivery reviews* **2007**. *59*. 1413-1433.
18. Khademhosseini, A., Vacanti, J.P., and Langer, R., Progress in tissue engineering. *Scientific American* **2009**. 300. 64-71.
19. Mao, H.Y., Laurent, S., Chen, W., Akhavan, O., Imani, M., Ashkarran, A.A., and Mahmoudi, M., Graphene: promises, facts, opportunities, and challenges in nanomedicine. *Chemical reviews* **2013**. *113*. 3407-3424.
20. Feng, L., Wu, L., and Qu, X., New horizons for diagnostics and therapeutic applications of graphene and graphene oxide. *Advanced Materials* **2013.** 25. 168-186.
21. Kim, J., Choi, K.S., Kim, Y., Lim, K.T., Seonwoo, H., Park, Y., Kim, D.H., Choung, P.H., Cho, C.S., and Kim, S.Y., Bioactive effects of graphene oxide cell culture substratum on structure and function of human adipose-derived stem cells. *Journal of Biomedical Materials Research Part A* **2013**. *101*. 3520-3530.
22. Heidari, M., Bahrami, H., and Ranjbar-Mohammadi, M., Fabrication, optimization and characterization of electrospun poly (caprolactone)/gelatin/graphene nanofibrous mats. *Materials Science and Engineering: C* **2017**. *78*. 218-229.
23. Jin, L., Wu, D., Kuddannaya, S., Zhang, Y., and Wang, Z., Fabrication, characterization, and biocompatibility of polymer cored reduced graphene oxide nanofibers. *ACS applied materials & interfaces* **2016**. *8*. 5170-5177.
24. Lim, K.T., Seonwoo, H., Choi, K.S., Jin, H., Jang, K.J., Kim, J., Kim, J.W., Kim, S.Y., Choung, P.H., and Chung, J.H., Pulsed-Electromagnetic-Field-Assisted Reduced Graphene Oxide Substrates for Multidifferentiation of Human Mesenchymal Stem Cells. *Advanced healthcare materials* **2016**. *5*. 2069-2079.
25. Dalby, M.J., Gadegaard, N., and Oreffo, R.O., Harnessing nanotopography and integrin–matrix interactions to influence stem cell fate. *Nature materials* **2014**. *13*. 558.
26. Kim, J., Bae, W.-G., Park, S., Kim, Y.J., Jo, I., Park, S., Jeon, N.L., Kwak, W., Cho, S., and Park, J., Engineering structures and functions of mesenchymal stem cells by suspended large-area graphene nanopatterns. *2D Materials* **2016**. *3*. 035013.
27. Seonwoo, H., Bae, W.-G., Park, S., Kim, H.-N., Choi, K.S., Lim, K.T., Hyun, H., Kim, J.-W., Kim, J., and Chung, J.H., Hierarchically micro-and nanopatterned topographical cues for modulation of cellular structure and function. *IEEE transactions on nanobioscience* **2016**. *15*. 835-842.